AIP | Journal of Applied Physics

Thermoelectric properties of Co0.9Fe0.1Sb3-based skutterudite nanocomposites with FeSb2 nanoinclusions

Chen Zhou, Jeffrey Sakamoto, Donald Morelli, Xiaoyuan Zhou, Guoyu Wang et al.

Citation: J. Appl. Phys. **109**, 063722 (2011); doi: 10.1063/1.3554403
View online: http://dx.doi.org/10.1063/1.3554403
View Table of Contents: http://jap.aip.org/resource/1/JAPIAU/v109/i6
Published by the AIP Publishing LLC.

Thermoelectric properties of $Co_{0.9}Fe_{0.1}Sb_3$-based skutterudite nanocomposites with $FeSb_2$ nanoinclusions

Chen Zhou,[1] Jeffrey Sakamoto,[1] Donald Morelli,[1,a)] Xiaoyuan Zhou,[2] Guoyu Wang,[2] and Ctirad Uher[2]
[1]*Department of Chemical Engineering and Materials Science, Michigan State University, East Lansing, Michigan 48824, USA*
[2]*Department of Physics, University of Michigan, Ann Arbor, Michigan 48109, USA*

(Received 20 September 2010; accepted 10 January 2011; published online 29 March 2011)

Bulk thermoelectric nanocomposite materials have great potential to exhibit higher figure of merit due to effects arising from the nanostructure. In this paper, we report thermoelectric properties from 80 K to 800 K of $Co_{0.9}Fe_{0.1}Sb_3$ based skutterudite nanocomposites containing $FeSb_2$ nanoinclusions. The nanoscale $FeSb_2$ precipitates are well dispersed in the skutterudite matrix and reduce the lattice thermal conductivity due to additional phonon scattering from the nanoscopic interfaces. Moreover, the nanocomposite samples also exhibit enhanced Seebeck coefficients relative to the regular iron substituted skutterudite samples. As a result, our best nanocomposite sample reached a dimensionless figure of merit of 0.59 at 788 K, a factor of two higher than that of the control sample $Co_{0.9}Fe_{0.1}Sb_3$. © *2011 American Institute of Physics*. [doi:10.1063/1.3554403]

I. INTRODUCTION

Persistent research efforts worldwide to develop thermoelectric (TE) materials are addressing the needs to develop alternative energy sources and improve efficiency of solid state cooling devices. Regardless of whether it is used in power generators or heat pumps, the performance of a TE material is characterized by the thermoelectric figure of merit (FOM) Z, which is defined by

$$Z = \frac{S^2\sigma}{\kappa},$$

where S is the Seebeck coefficient (also known as the thermopower), σ the electrical conductivity, and κ the thermal conductivity. The numerator $S^2\sigma$ is called the TE power factor. As Z is often a function of temperature, it has become a common practice to use the dimensionless FOM ZT in place of Z where T is the mean operating temperature. The higher the ZT, the better a TE performance a material possesses.

Skutterudite compounds were identified as good candidates for thermoelectric application almost two decades ago.[1] Unfilled skutterudites are binary compounds of the form MA_3, where M is a metal such as Co, Rh, or Ir, and A is As, P, or Sb.[2,3] The high carrier mobility and large effective mass found[4,5] in some skutterudites endow them with power factors comparable to and even exceeding Bi_2Te_3 and PbTe. Their thermal conductivities, on the other hand, are relatively large to make them useful TE materials.[5,6] Previous attempts at reducing thermal conductivity focused on inserting foreign atoms into the large voids in the unfilled skutterudite structure, thus producing "filled" skutterudite compounds.[7–9] The foreign atom confined in the cage exhibits an Einsteinlike mode that provides additional phonon scattering to dampen the lattice thermal conductivity.[6,10,11] This approach has achieved great success especially in enhancing the ZT in n-type filled skutterudites, for instance, it is not unusual for double-filled skutterudites to display[12] ZT greater than 1.3, and the melt-spun filled skutterudites containing InSb nanoinclusions reaching[13] ZT in excess of 1.4. Recently, even p-type filled skutterudites exceeded ZT of unity.[14]

Another direction originating from a different train of thought for improving the TE properties is to reduce the dimension of materials' building block, also referred to as "nanostructuring." The physics is either to evoke quantum confinement in order to alter the density of states (DOS)[15] or to tweak the carrier scattering parameter so that one may have the chance to boost the Seebeck coefficient, and hence the power factor.[16] The thermal conductivity is also expected to be reduced because of the extra phonon scattering from the myriad of nanoscopic interfaces.

In this paper, we report work on bulk p-type skutterudite nanocomposites of $Co_{0.9}Fe_{0.1+x}Sb_{3+2x}$. This composition can be reformulated as a base composition of $Co_{0.9}Fe_{0.1}Sb_3$ and a variant part of $FeSb_2$. It is our interest to initially demonstrate whether these nanocomposites can be synthesized and, if so, whether the existence of nanoinclusions can offer any positive influence. Four samples were synthesized with $x = 0$, 0.05, 0.1, and 0.2 respectively. A fifth sample was fabricated with composition $Co_{0.75}Fe_{0.25}Sb_3$ that has the same Fe/Co ratio as that of $x = 0.2$ sample. Here $x = 0$ and $Co_{0.75}Fe_{0.25}Sb_3$ both serve as control groups to discern if property changes are related to Fe substitution for Co or $FeSb_2$ nanoinclusions.

II. EXPERIMENT

High purity starting materials of Co (powder 99.5%), Fe (powder 99%), and Sb (lump 99.999%) were weighed according to the stoichiometric ratio and charged into carbon coated ampoules. The ampoules were sealed under vacuum of 10^{-6} Torr, heated at 1100C for three hs to melt the

a)Author to whom correspondence should be addressed. Electronic mail: dmorelli@egr.msu.edu.

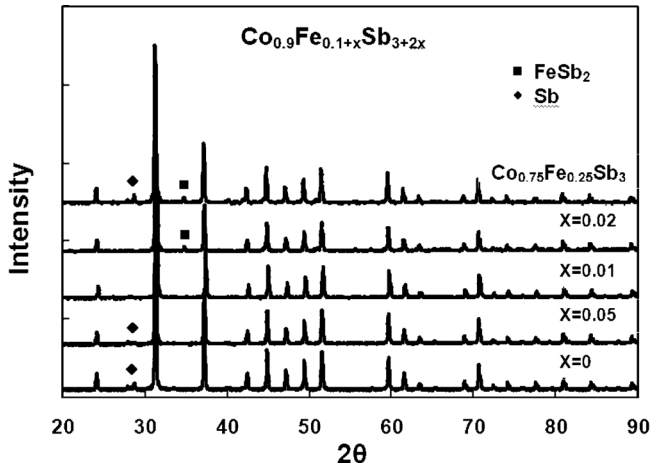

FIG. 1. X-ray diffractions of samples x=0, 0.05, 0.1, 0.2 and control sample $Co_{0.75}Fe_{0.25}Sb_3$.

materials and rapidly quenched in a cold water bath. The quenched samples were annealed at 700C for three days.

A disk was cut from the middle of each ingot and further sectioned into rectangular parallelepiped with dimensions of approximately 3 mm × 3 mm × 8 mm for measuring transport properties from 80 K to 300 K. Seebeck coefficient, electrical resistivity, and thermal conductivity were measured from 80 K to 300 K under vacuum using a steady state technique in a continuous flow cryostat with liquid nitrogen as a refrigerant. The accuracy of the electrical resistivity and thermal conductivity measurement is limited by the precision in measuring dimensions of samples, namely, the distance between two thermocouple probes and the cross-sectional area. They are also affected by the thermal and electrical contacts between thermocouple probes and sample, which also applies to measurements of the Seebeck coefficient. We estimate a 10% uncertainty in transport properties measurement from 80 K–300 K.

A thin slab of approximate thickness of 1mm was cut out of the same low temperature measurement sample for Hall measurement. Hall coefficients and electrical resistivity from 60 K to 400 K were carried out using ac current in a varying magnetic field from −3T to 3T. The remnants from the disks were pulverized to powders for x-ray diffraction analysis and/or mounted on conducting epoxy for scanning electron microscope (SEM) imaging. X-ray diffraction patterns for all samples were collected from 2θ ranging from 20 to 90 degrees in a Rigaku MiniFlex 2 using Cu Kα radiation. SEM images were done in JEOL Corporation model JSM 7500 high resolution field emission SEM.

High temperature electrical conductivity and the Seebeck coefficient were measured in the interval 300 K – 800 K using a home built apparatus under the protective atmosphere of argon on the same rectangular samples measured at temperatures below the ambient. Separate disks sectioned from individual ingots in proximity to where rectangular samples were cut were used for high temperature thermal conductivity measurements. Thermal conductivity was obtained from measurements of thermal diffusivity (Anter, Flashline 5000), specific heat (Netzsch, 404 Pegasus), and density (Archimedes' law).

III. RESULTS

Figure 1 displays our x-ray diffraction results, which show that the skutterudite phase is the majority phase for all samples. A minute amount of Sb impurity phase is present in samples with $x = 0$, $x = 0.05$, and the control sample $Co_{0.75}Fe_{0.25}Sb_3$. As anticipated, the $FeSb_2$ phase can be found in samples with high Fe content, $x = 0.2$ and $Co_{0.75}Fe_{0.25}Sb_3$.

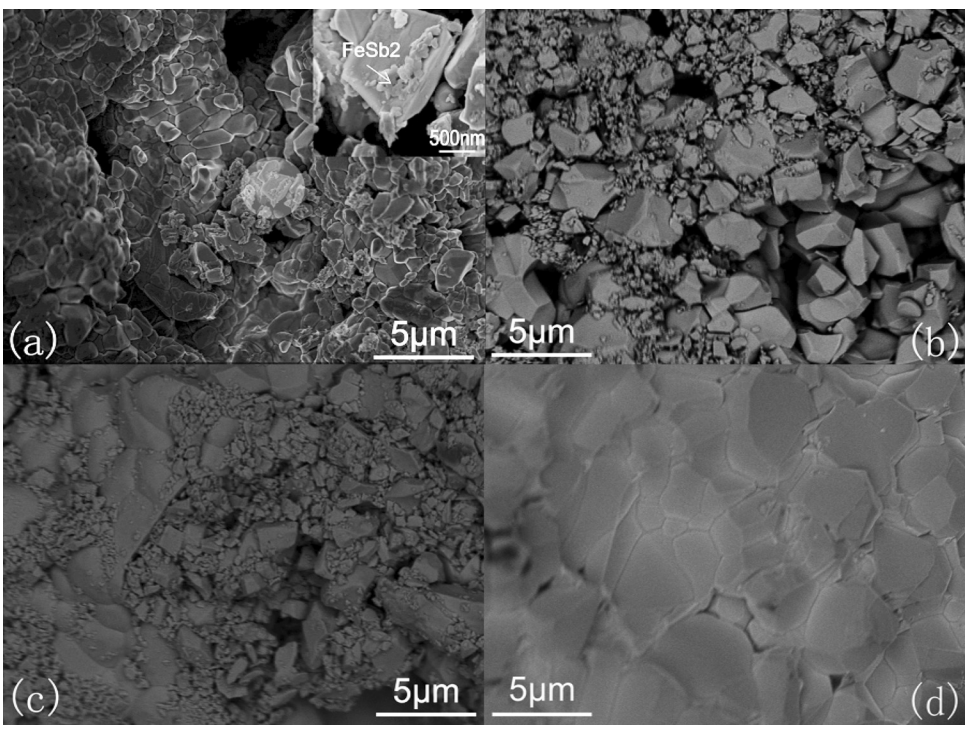

FIG. 2. High resolution FESEM images on fractured surface of nanocomposite samples $Co_{0.9}Fe_{0.1}Sb_3$+x$FeSb_2$ and control sample $Co_{0.75}Fe_{0.25}Sb_3$. (a) x=0.05, the inset image zooms in the circled area to reveal the nanoscopic feature; (b) x=0.1; (c) x=0.2; (d) $Co_{0.75}Fe_{0.25}Sb_3$.

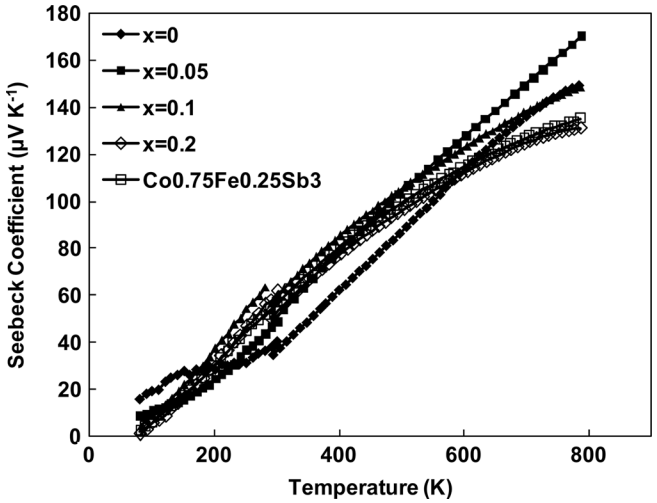

FIG. 3. Seebeck coefficient as a function of temperature.

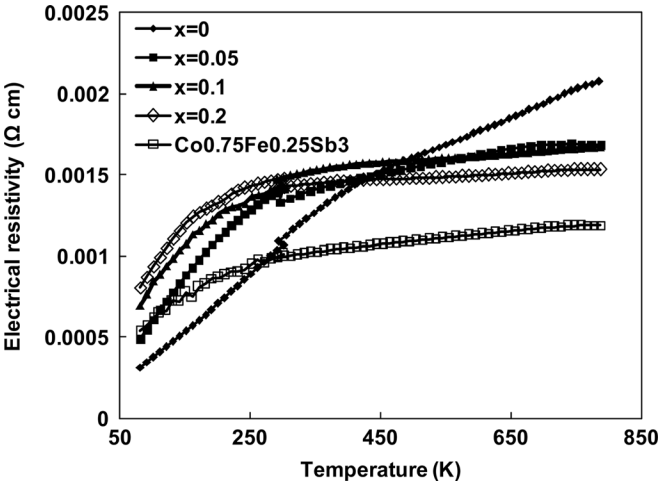

FIG. 4. Electrical resistivity as a function of temperature.

Figure 2 shows high resolution FESEM images of all nanocomposite samples ($x = 0.05$, $x = 0.1$, $x = 0.2$), and control sample $Co_{0.75}Fe_{0.25}Sb_3$. The amount of nanoparticles present in the SEM images approximately scales with the $FeSb_2$ we intentionally added to the base composition $Co_{0.9}Fe_{0.1}Sb_3$ as shown from Figs. 2(a)–2(c). In Fig. 2(d), which retains the same Fe/Co ratio as $x = 0.2$ sample but has the normal skutterudite composition MA_3, the nanoparticles have almost disappeared and grain boundaries are much cleaner compared to nanocomposite samples. This suggests that either Fe atoms were absorbed to form skutterudite or some $FeSb_2$ nanoparticles have grown up significantly to micron size. We also performed the energy dispersive x-ray spectroscopy (EDS) analysis in the same region as shown in Fig. 2(b). By using "Point and ID Analyzer" function, we detected higher Fe but less Sb content at the place with cluster of nanoparticles compared to the skutterudite grains without such features. Combined with x-ray diffraction results, we identified the nanoinclusions observed in our SEM images to be $FeSb_2$.

The Seebeck coefficient as a function of temperature is plotted in Fig. 3. Here, in order to compare their properties, we also include the results of $Co_{0.9}Fe_{0.1}Sb_3$ from the literature.[17] All Seebeck coefficients increase monotonously with increasing temperature. Our base sample $x = 0$ exhibits a very similar behavior to that of the reference. All nanocomposite samples and the higher Fe content control sample $Co_{0.75}Fe_{0.25}Sb_3$ exhibit higher Seebeck coefficients than the $x = 0$ sample between 160 K and 565 K. Samples $x = 0.05$ and $x = 0.01$ extend the lead all the way up to the measurement limit at 788 K. The Seebeck coefficients for the nanocomposite samples first increase with the amount of $FeSb_2$ (when x is less than 0.1) and then start to drop for samples with higher amount of $FeSb_2$.

The electrical resistivity as a function of temperature is shown in Fig. 4. The resistivity for all samples exhibits a metallic behavior, increasing with temperature. Nanocomposites have higher resistivity values than the control sample $x = 0$ at lower temperature, but, interestingly, they begin to saturate near room temperature, a behavior that is not observed in the sample with $x = 0$. The crossover happens around 423 K. Above 500 K sample $x = 0$ has the largest electrical resistivity. $Co_{0.75}Fe_{0.25}Sb_3$ has the lowest resistivity, a phenomenon to be expected as the higher Fe substitution creates more holes, but it also exhibits the saturation behavior similar to the nanocomposite samples. The temperature dependence of power factor is displayed in Fig. 5. All nanocomposite samples have higher power factors compared to control sample $x = 0$. Sample $x = 0.05$ shows the highest value of 17×10^{-6} $Wcm^{-1}K^{-2}$ at 788 K.

The temperature dependence of the thermal conductivity is plotted in Fig. 6. The thermal conductivity in all nanocomposite samples is substantially reduced with respect to the both control sample $x = 0$ and $Co_{0.75}Fe_{0.25}Sb_3$ over the whole temperature range of measurement, and is even comparable to some filled skutterudites.[18]

Mismatches between low and high temperature data sets at 300 K for some samples do exist in electrical resistivity as well as thermal conductivity as shown in Fig. 4 and Fig. 6 respectively. The difference in resistivity is less than 6% for all samples. The largest difference in thermal conductivity is about 24% found in $x = 0$ sample. We estimate the error is inherent to the geometric factor used for computing electrical resistivity and, in the case of thermal conductivity, due to

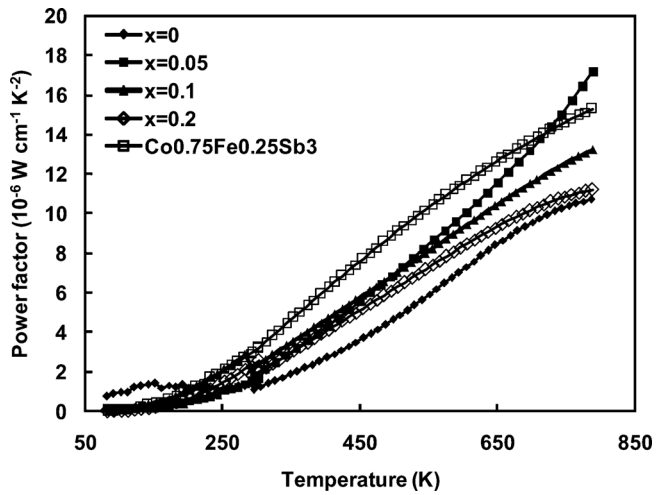

FIG. 5. Temperature dependence of the power factor.

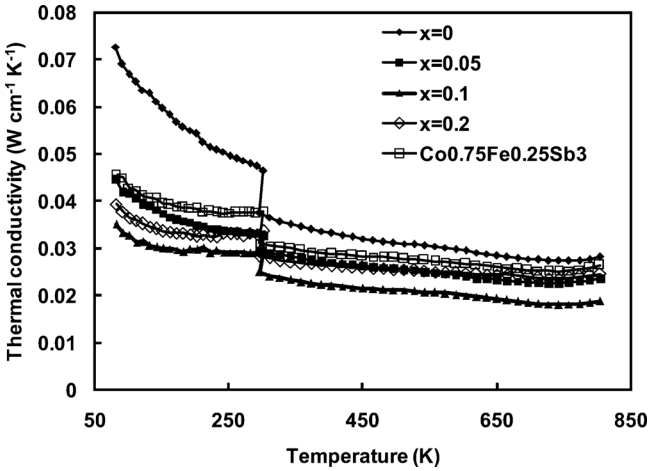

FIG. 6. Thermal conductivity as a function of temperature.

different techniques used to determine thermal conductivity at low and high temperatures. The overall effect on ZT, however, is insignificant as the errors from resistivity and thermal conductivity partially cancel out each other. The combined enhancement of power factors and the reduction in thermal conductivity in our nanocomposites increase the ZT values compared to the control sample $x = 0$ as shown in Fig. 7. Sample $x = 0.05$ displays a ZT=0.59 at 788 K which is twice as large as that of sample $x = 0$, and shows no sign of reaching its peak at the limiting temperature of these measurements.

IV. DISCUSSION

It is imperative to discern the influence of Fe substitution and justify that the enhancement of TE properties can be attributed to the $FeSb_2$ nanoinclusions. To do so, we have calculated the lattice constant based on the d-value corresponding to plane (631) as a function of Fe ratio on the metal site. Upon Fe replacement of Co, the lattice constant is expected to increase linearly with the Fe concentration. This is indeed the case for our samples that satisfy the skutterudite formula MA_3. The lattice constants for the nanocomposites, on the other hand, first expand slightly compared to the control sample $x = 0$, but eventually saturate with additional Fe content. This is a strong indication of the formation of $FeSb_2$ precipitates. For the $Co_{0.75}Fe_{0.25}Sb_3$ sample, the lattice constant is smaller than the value of 9.062 Å reported on the same composition.[19] So the actual amount of Fe going into the Co sites may be smaller than the stoichiometric amount, with the remaining Fe atoms combining with excess Sb to form $FeSb_2$.[20]

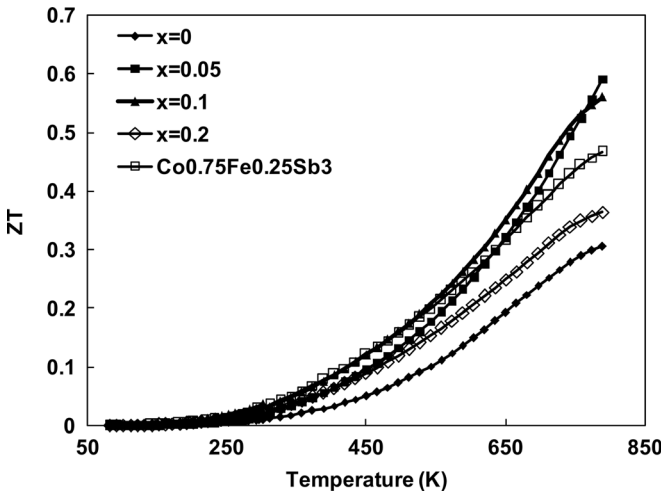

FIG. 7. ZT as a function of temperature.

As Fe has one less valence electron than Co, Fe substitution for Co will increase the hole concentration. Thus given the same carrier scattering parameter λ (which determines the energy dependence E of the carrier scattering time via the relation $\tau \sim E^{\lambda}$), the Seebeck coefficient should decrease with an increasing Fe substitution due to the increase of hole concentration. The data reported by Tang *et al.* on $Fe_xCo_{4-x}Sb_{12}$ supports this assumption quite well.[19] Our control sample $x = 0$ also agrees reasonably well with the fitted line based on Tang's data. The thermopowers for the nanocomposites diverge from the fit line for regular Fe substituted samples, which suggest the enhanced thermopower is due to an alteration in the scattering parameter λ brought about by the $FeSb_2$ nanoinclusions.[16] The other control sample $Co_{0.75}Fe_{0.25}Sb_3$ also diverges from the fit. Combining the analysis of the lattice constant and the behavior of the thermopower described above, we believe that trace $FeSb_2$ nanoparticles must have formed in this sample too, influencing its properties.[20]

V. CONCLUSION

We have successfully synthesized p-type skutterudite nanocomposites based on $Co_{0.9}Fe_{0.1}Sb_3$ with $FeSb_2$ nanoinclusions. The existence of $FeSb_2$ nanoparticles not only provides extra phonon scattering that reduces the thermal conductivity, but also changes the hole scattering parameter resulting in an enhanced thermopower and power factors in $x = 0.05$ and $x = 0.1$ samples. The best nanocomposite sample displays a $ZT = 0.59$ at 788 K, which is a factor of two increase compared to the control sample $x = 0$. Considering the prototype of the base material is Fe doped binary skutterudite, nanocomposite synthesis is a very promising approach for improving TE properties.

ACKNOWLEDGMENTS

This work is supported by the State of Michigan under University Research Corridor seed Grant. Sample synthesis and characterization are partially supported as part of the Revolutionary Materials for Solid State Energy Conversion, an Energy Frontier Research Center funded by the US Department of Energy, Office of Science, Office of Basic Energy Science under Award Number DE-SC001054. The authors thank Dr. Taolin Ren and Chang Liu for SEM assistance.

[1]T. Caillat, A. Borshchevsky, and J.-P. Fleurial, in *Proceedings of the 11th International Conference on Thermoelectrics, Arlington, Texas, 1992*, edited by K. R. Rao (The University of Texas at Arlington, Arlington, TX, 1992), p. 276.
[2]G. S. Nolas, D. T. Morelli, and T. M. Tritt, Annu. Rev. Mater. Sci. **29**, 89 (1999).
[3]C. Uher, in *Semiconductors and Semimetals*, edited by T. Tritt (Academic Press, San Diego, 2001), Vol. 69, p. 139.
[4]D. T. Morelli, G. P. Meisner, B. X. Chen, S. Q. Hu, and C. Uher, Phys. Rev. B **56**, 7376 (1997).

[5]B. X. Chen, J. H. Xu, C. Uher, D. T. Morelli, G. P. Meisner, J. P. Fleurial, T. Caillat, and A. Borshchevsky, Phys. Rev. B **55**, 1476 (1997).
[6]D. T. Morelli and G. P. Meisner, J. Appl. Phys. **77**, 3777 (1995).
[7]D. J. Braun and W. Jeitschko, J. Less-Common Met. **72**, 147 (1980).
[8]D. J. Braun and W. Jeitschko, J. Solid State Chem. **32**, 357 (1980).
[9]W. Jeitschko and D. J. Braun, Acta Crystallogr. **B33**, 3401 (1977).
[10]G. A. Slack, in *CRC Handbook of Thermoelectrics*, edited by D. E. Rowe (CRC Press, Boca Raton, FL, 1995), p. 407.
[11]B. C. Sales, D. Mandrus, and R. K. Williams, Science **272**, 1325 (1996).
[12]X. Shi, H. Kong, C. P. Li, C. Uher, J. Yang, J. R. Salvador, H. Wang, L. Chen, and W. Zhang, Appl. Phys. Lett. **92**, 182101 (2008).
[13]H. Li, X. Tang, Q. Zhang, and C. Uher, Appl. Phys. Lett. **94**, 102114 (2009).
[14]G. Rogl, A. Grytsiv, E. Bauer, P. Rogl, and M. Zehetbauer, Intermetallics **18**, 57 (2010).
[15]G. Chen, M. S. Dresselhaus, G. Dresselhaus, J. P. Fleurial, and T. Caillat, Int. Mater. Rev. **48**, 45 (2003).
[16]J. P. Heremans, C. M. Thrush, and D. T. Morelli, Phys. Rev. B **70**, 115334 (2004).
[17]J. Yang, G. P. Meisner, D. T. Morelli, and C. Uher, Phys. Rev. B **63**, 014410 (2001).
[18]J. R. Salvador, J. Yang, X. Shi, H. Wang, A. A. Wereszczak, H. Kong, and C. Uher, Philos. Mag. **89**, 1517 (2009).
[19]X. F. Tang, L. D. Chen, G. Takashi, H. Toshio, and R. Z. Yuan, Acta Phys. Sin. **49**, 1120 (2000).
[20]C. Zhou, J. Sakamoto, and D. Morelli, "Low temperature thermoelectric properties of $Co_{0.9}Fe_{0.1}Sb_3$-based skutterudite based nanocomposites with $FeSb_2$ inclusions," J. Electron. Mater. (to be published).